

Precipitation polymerisation of vinylidene fluoride in supercritical CO₂ and real-time calorimetric monitoring

Jun Liu, Hongyun Tai, Steven M. Howdle*

School of Chemistry, University of Nottingham, University Park, Nottingham NG7 2RD, UK

Received 23 August 2004; received in revised form 5 December 2004; accepted 6 December 2004

Available online 11 January 2005

Abstract

Vinylidene fluoride was polymerised in supercritical carbon dioxide. Power compensation calorimetry was used to monitor the polymerisation process on-line. The polymer product was found to have a low apparent-density, leading to an observed high solid content in the autoclave at low yields. In situ calorimetry showed a sharp transition of the heat transfer in the reactor, leading to a useful parameter for monitoring the polymerisation process. The stirring rate was found to have no effect on the molecular weight, but did modify the calorimetric traces and the morphology of the polymer. The polymerisation at a lower pressure resulted in a lower molecular weight product and a lower polymerisation rate.

© 2004 Elsevier Ltd. All rights reserved.

Keywords: Vinylidene fluoride; Polymerisation; Calorimetry

1. Introduction

Poly(vinylidene fluoride) (PVDF) and its copolymers are important fluoropolymers, which exhibit the unique combination of excellent chemical resistance, high thermal stability, desirable mechanical and surface properties, good piezoelectric and pyroelectric properties, low water absorptivity, excellent weatherability and low flammability [1,2]. Because of these properties, PVDF is widely used as wire and cable insulation, tubing, fittings, valves and pumps [1]. Commercial PVDF is usually produced by free radical emulsion and suspension polymerisations [3–6], both of which generate large quantities of wastewater and require substantial quantities of energy to dry the polymer product.

Supercritical carbon dioxide (scCO₂) is an environmentally acceptable alternative solvent. It has a unique combination of liquid and gas like properties and has been widely applied as a green solvent for extraction, material preparation and catalysis [7,8]. It has also been used as a

solvent for polymer synthesis and processing although most polymers are insoluble in scCO₂ [9–12]. From an industrial perspective, CO₂ is inexpensive, non-toxic, non-flammable, and readily available in high purity from a variety of sources. Polymers can be isolated from the reaction mixture by a simple depressurisation, resulting in a clean, dry polymer product. This eliminates the necessity for energy-intensive drying procedures often required in the polymer manufacture. Previous studies have reported the thermally initiated continuous polymerisation [13] and γ -radiation-initiated polymerisation of vinylidene fluoride (VDF) in scCO₂ [14]. The copolymerisation of VDF with vinyl acetate in scCO₂ was also reported recently [15,16].

Most physical and chemical processes are accompanied by a heat change. Therefore calorimetry is a powerful tool to monitor these processes. The use of reaction calorimetry in polymerisations has been widely explored [17,18]. However, most calorimetric studies have been carried out at ambient or low pressures. We have used power compensation isothermal calorimetry (PCIC) to monitor the polymerisation of methyl methacrylate and glycidyl methacrylate in scCO₂ [19,20]. In this paper we explore whether the calorimetry can be used to monitor the precipitation polymerisation of VDF in scCO₂ on-line.

* Corresponding author. Tel.: +44 11 5951 3058; fax: +44 11 5951 3058.

E-mail address: steve.howdle@nottingham.ac.uk (S.M. Howdle).

2. Experimental

2.1. Materials

VDF was kindly donated by Solvay Research (Belgium) and used without further purification. High purity carbon dioxide (BOC Gases, SFC Grade) was used as received. The initiator diethyl peroxydicarbonate (DEPDC) was synthesised according to the literature [21] and used as a solution of approximately 10 wt % DEPDC in 1,1,1,3,3-pentafluorobutane (PFB) (SOLKANE® 365 MFC, Solvay Research, Belgium). The initiator solutions were carefully stored in a freezer at $-15\text{ }^{\circ}\text{C}$.

2.2. Polymerisation

The experimental set-up is shown in Fig. 1. Polymerisations were conducted in a 60 ml stainless steel autoclave fitted with a magnetically coupled overhead stirrer with a simple ‘paddle’ blade [22,23] and motorized driver. A thermocouple was inserted directly into the autoclave, which provided an accurate temperature measurement of the reaction fluid. A heating jacket connected to a circulating oil thermostat (JulaboF32-HD, JULABO Labortechnik GmbH) was used to control the temperature to $2\text{ }^{\circ}\text{C}$ lower than the required reaction temperature. Simultaneously, an internal heater (6 in Fig. 1) was also used to control the temperature of the reaction mixture. The power output of the internal heater was controlled and monitored by the HEL auto-mate electronics and software (Hazard Evaluation Laboratory) [19,20]. The temperature and pressure of the reaction was also logged automatically.

In a typical polymerisation, the autoclave was pressurized to ca 3000 psi (20.41 MPa) with oxygen-free nitrogen to leak test and degas the system. After venting the nitrogen, the monomer VDF was transferred into the autoclave from a sample cylinder of known volume and weight. CO_2 was pumped into the autoclave to 860 psi (5.85 MPa) at room temperature. The autoclave was then heated to reaction

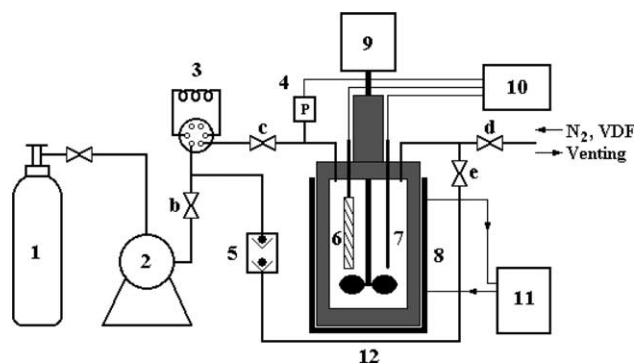


Fig. 1. The schematic of polymerisation apparatus. 1, CO_2 cylinder; 2, Pickel pump (PM101); 3, initiator sample loop; 4, pressure transducer; 5, Gilson pump; 6, internal heater; 7, thermocouple; 8, heating jacket; 9, stirrer driver; 10, HEL auto-mate interface; 11, Julabo refrigerated and heating circulator; 12, autoclave; a, b, c, d and e, valves.

temperature and pressurized with additional CO_2 to the desired working pressure. The initiator solution was transferred via a syringe into a small sample loop (0.5 ml, 3 in Fig. 1) after which the valve b in Fig. 1 was closed. A Gilson 302 pump (5 in Fig. 1) was used to circulate this initiator solution into the autoclave whilst keeping the pressure constant. The flow rate of CO_2 was set to 2 ml min^{-1} and the solution was metered in over a period of 5 min. After the reaction, the CO_2 was vented slowly. The solid polymer was collected and the yield was measured gravimetrically.

Visual observation of the polymerisation was carried out in a stainless steel autoclave fitted with a sapphire window [24]. The autoclave has a volume of 100 ml and is fitted with a magnetically coupled overhead stirrer with a simple ‘paddle’ blade which is same as the stirrer in the autoclave used to carry out the polymerisation.

2.3. Polymer characterisation

Molecular weight data were obtained by gel permeation chromatography (GPC) on a Polymer Laboratories GPC system with 2 MIXED-C columns at $80\text{ }^{\circ}\text{C}$, using *N,N*-dimethylformamide (DMF) modified with 0.1 mol l^{-1} LiBr as eluent. The flow rate was 1 ml min^{-1} . The GPC was calibrated at $80\text{ }^{\circ}\text{C}$ using narrow molecular weight distribution standards of poly(methyl methacrylate) purchased from Polymer Laboratories Ltd. Scanning electron microscopy (SEM) data were collected using a JEOL 6400 SEM. Samples were mounted on an aluminium stub using an adhesive carbon tab and were gold coated.

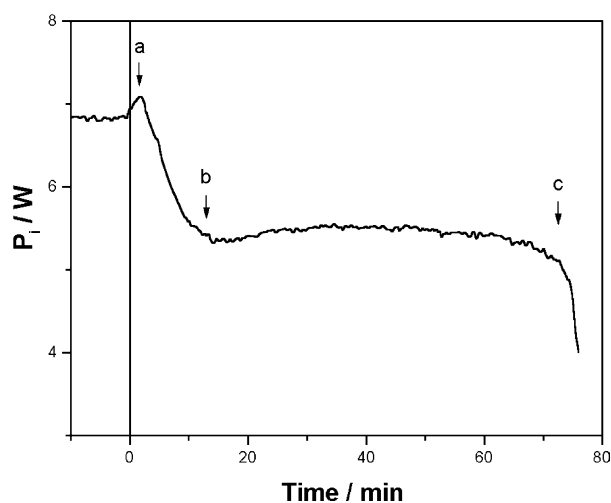


Fig. 2. A typical power trace of VDF precipitation polymerisation in scCO_2 . Note that equilibrium conditions are verified before injection of initiator (point a) and subsequently a plateau level (b) is reached before a second abrupt decrease in heater power (c). Experimental detail is listed in Table 1, entry 2.

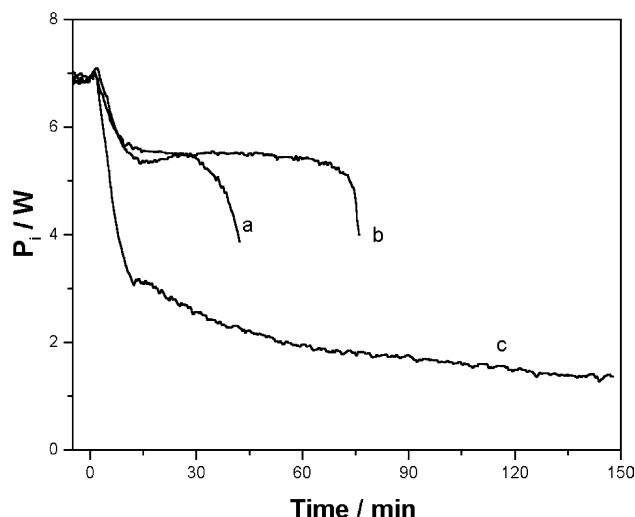


Fig. 3. The power traces of VDF precipitation polymerisation with different stirring rate. (a) 700 rpm; (b) 300 rpm; (c) 50 rpm.

3. Results and discussions

3.1. Principle of power compensation isothermal calorimetry

Power compensation isothermal calorimetry is a method of maintaining constant temperature of the system by adjusting the power output of the internal heater. At the same time, the heat exchange between the reaction system and heating jacket (8 in Fig. 1) was kept constant by maintaining a constant temperature difference. The general energy balance is:

$$P_i = UA(T_r - T_j) + C_p \frac{dT_r}{dt} - Q_r \quad (1)$$

where Q_r is the rate of heat generation from the polymerisation, U is the heat transfer coefficient between the reaction system and the heating jacket, A is the area of heat transfer, T_r is the reaction temperature, T_j is the jacket temperature which is controlled to be lower than T_r . C_p is the heat capacity of the reaction mixture and P_i is the power of the internal heater. The first term on the right of Eq. (1) is the heat flow through the reactor wall. And the second term is the accumulation of enthalpy in the reactor. Because both the reaction temperature and the jacket temperature are kept constant, the accumulation of enthalpy in the reactor is negligible, and $\Delta T = T_r - T_j$ is constant. So Eq. (1) can be simplified as:

$$Q_r = UA(T_r - T_j) - P_i = UA\Delta T - P_i \quad (2)$$

Because there is no reaction at $t=0$, $Q_{r,0}=0$,

$$Q_{r,0} = 0 = U_0A\Delta T - P_{i,0} \quad (3)$$

If U is constant in the reaction process, i.e. $U=U_0$, then $UA\Delta T=P_{i,0}$. So,

$$Q_r = P_{i,0} - P_i \quad (4)$$

Therefore, Q_r can be monitored by recording the change of P_i .

3.2. Monitoring of the polymerisation process

DEPDC was used as the initiator. Its decomposition rate constant from 65 to 85 °C is available from literature [25]. In this work, polymerisation was carried out at 55 °C. The decomposition rate constant of DEPDC at 55 °C was extrapolated from the data of 65–85 °C with Arrhenius equation. It is $2.77 \times 10^{-5} \text{ s}^{-1}$ which corresponds to a half-life of 6.95 h.

VDF is completely miscible with scCO_2 . The reaction mixture is homogeneous at the start of the reaction but solid particles appear almost immediately after the injection of initiator in the visual test carried out in the view cell. As the polymerisation proceeds the solid content increased gradually.

Figure 2 shows the power trace of a typical polymerisation process at 55 °C. The concentrations of initiator and VDF, and stirring rate are listed in Table 1, entry 2. Before the injection of initiator, the power was shown to be constant. About 2–3 min after the injection of the initiator (Fig. 2, point a), the power to the internal heater (P_i) began to decrease because of the polymerisation exotherm. After ca 10 min (Fig. 2, point b), this value then reached a plateau. After a further 70 min (Fig. 2, point c), the P_i decreased abruptly. This second decrease in power from the internal heater may be ascribed to the autoclave becoming full of polymer solid. Prior to this, stirring within the autoclave was effective in mixing the reactor contents and the heat from the exotherm was efficiently transferred between the reaction mixture and the reactor wall via convection. However, once the cell was full of polymer, stirring was no longer effective and the rate of thermal exchange between the reactor wall and the reaction mixture decreased. This caused the thermal flow through the reactor wall to decrease and as a result, whilst Q_r was constant, the P_i decreased because of decreased thermal loss from the autoclave. Therefore the second drop in the power from the internal heater is a clear indication of the build up of a substantial solid content within the autoclave. From an operational point of view this information is crucially important in demonstrating the point at which reactor fouling might begin to occur, heat transfer from the vessel becomes inefficient, and large fluctuations in reactor temperature and pressure would be seen.

We carried out some polymerisations to times beyond point c. In these experiments, the temperature after point c fluctuated much more than before point c. Specifically before point c, the temperature was controlled within less than ± 0.05 °C. However after point c, the temperature fluctuation could be as large as ± 0.5 °C. Such a situation might lead to inefficient heat transfer and the potential for undesirable increase in pressure.

To confirm the assumption that the autoclave was full of

polymer solid which causes the second decrease in power in Fig. 2 (point c), experiments were performed in a view cell. In these experiments, stirring rates were fixed at 300 rpm. After the autoclave was full, the polymerisation was terminated by switching off heating power and venting CO₂ and monomer. Intriguingly, the yield of materials obtained was reproducibly in the range ca 2 g, corresponding to a very low conversion of ca 20% and demonstrating an extremely low apparent-density of 2 g polymer in 60 ml volume. The published value for the density of PVDF is in the range of 1.75–1.78 g ml⁻¹ depending on the crystallinity [1]. The apparent-density of the PVDF obtained in these scCO₂ experiments appears much lower, mainly because the polymer appears to be porous (Fig. 4). Also, PVDF is a semi-crystalline polymer. The polymer particles are solid after crystallisation and do not agglomerate. As a result, the PVDF particles are loosely stacked in the reactor leading to the observed low apparent-density.

One might expect that the swelling of the PVDF by CO₂ might also partly contribute to the low apparent-density. It is well known that scCO₂ does swell amorphous polymers and the amorphous regions of semi-crystalline polymers [9,26]. Although, under our experimental conditions, the linear elongation of PVDF in a scCO₂ atmosphere was reported to be only about 1% [27,28], the presence of monomer could also contribute to some swelling of the polymer.

3.3. The effect of stirring rate

Our previous work showed that the stirring rate had no significant effect upon molecular weight. However, stirring had a strong effect on the particle morphology. Experimental results indicated that the shear force of the agitation could induce break-up of the primary particles [29]. The calorimetric monitoring technique was employed here to investigate the effect of stirring. Polymerisations were carried out at a range of different stirring rates from 300 to 700 rpm. By calorimetric monitoring, we observed that the point at which the autoclave became full of PVDF was found to depend strongly upon the stirring rate. This point occurs much earlier under 700 rpm stirring (entry 3 in Table 1 and curve a in Fig. 3). With a lower stirring rate (50 rpm, entry 1 of Table 1), the second power drop did not appear

even after a much longer reaction time of 150 min. However, the power from the internal heater did appear to show a continual steady drift probably indicating fouling of the reactor wall by the polymer. From Eq. (1), one can relate this to the steady decrease of the heat transfer coefficient U leading to a continuous decrease of P_i .

The rate of polymerisation was found to increase with the stirring rate, whilst there was no significant change in the molecular weight or polydispersity. This might be related to the higher diffusibility of the monomer into the polymer particles under a higher stirring rate. The effect of stirring rate on the polymerisation rate and upon molecular weight agrees with published data from the continuous precipitation polymerisation [30] of VDF in scCO₂.

The stirring rate can strongly affect the crystallisation process. It was reported that flow or shear could induce the acceleration of crystallisation and the formation of anisotropic crystallites in the melt phase crystallisation process [31–34]. For example, Kornfield et al. reported the flow-induced formation of oriented, thread-like nuclei and the acceleration of the crystallisation rate [31]; and Acierno et al. reported the transition from a low-shear rate isotropic morphology to a high-shear rate rod-like crystalline structure [32]. In our system, it is also expected that the high stirring rate will induce the formation of thread-like nuclei and increase the crystallisation rate. A faster crystallisation rate will result in smaller, harder particles and less agglomeration. As a consequence, the particles will be stacked more loosely and the apparent density will be lower. Thus, the calorimetric power profiles appear to follow these trends. The morphology of the PVDF powder obtained (Fig. 4) demonstrates that as one might expect, the polymer is more porous at higher stirring rates. The lower stirring rate leads to larger spherical particles, whilst under high stirring rates the particles were more fibre-like or thread-like. (Fig. 4)

3.4. The effect of pressure

The density and the solvent characteristics of scCO₂ are pressure dependent. The variation of pressure is known to exert a strong effect upon the polymerisation process; not only the polymerisation kinetics, but also the swelling of the

Table 1
The precipitation polymerisation of VDF in supercritical CO₂ under different conditions

No	C_M^a (mol l ⁻¹)	SR ^b (rpm)	Time (min)	P (psi)	Yields (g)	Conv. ^c (%)	R_p^d (g min ⁻¹ l ⁻¹)	M_w (kg mol ⁻¹)	PDI
1	3.0	50	148	4000	3.08	26.7	0.347	34.5	1.59
2	2.6	300	76	4000	1.94	19.8	0.425	36.8	1.46
3	2.6	700	42	4000	1.20	12.1	0.476	38.5	1.69
4	3.1	300	112	1800	1.89	15.9	0.281	20.9	1.44

The polymerisation condition: $T=55$ °C, initiator concentration 7.5 mmol l⁻¹, reactor volume 60 ml.

^a Monomer concentration.

^b Stirring rate.

^c Conversion.

^d Rate of polymerisation.

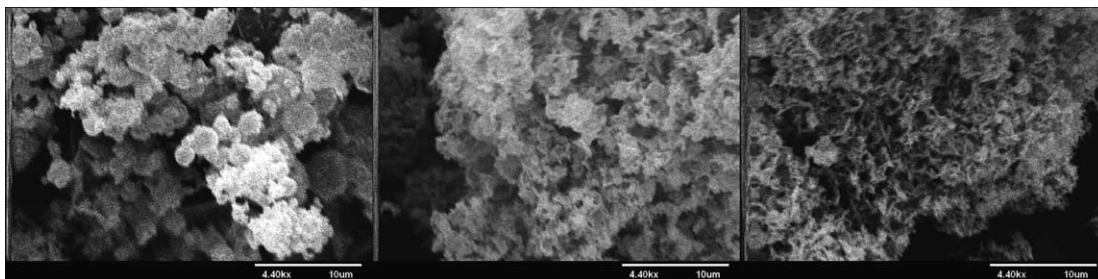


Fig. 4. SEM of PVDF polymerised under different stirring rate. From left to right the stirring rate was 50, 300, 700 rpm, respectively.

polymer product and morphology. For polystyrene, dispersion polymerisations carried out under a series of different pressures (140–439 bar) resulted in a large effect upon the conversion, molecular weight, and PS particle diameter, suggesting that the polymerisation of PS in scCO_2 is extremely sensitive to the density of the continuous phase [35]. Very similar effects have been reported for the observed particle diameters of the dispersion polymerisation of acrylonitrile [36], HEMA [37] and GMA [38]. Our previous work has also demonstrated that the density has a dramatic effect in the final product morphology in the dispersion polymerisation of GMA [20].

For PVDF, it has been reported that an increase of pressure increases the molecular weight and polydispersity of PVDF by a continuous polymerisation process [30,39]. Our data obtained by the batch process show similar results (Table 1 entries 4 and 2), also at lower pressures (1800 psi, 12.24 MPa) a lower molecular weight and lower polymerisation rate are observed. At 55 °C, the calculated densities [40] are dramatically different for pure CO_2 (1800 psi (12.24 MPa); 0.54 g ml^{-1} and 4000 psi (27.21 MPa); 0.83 g ml^{-1}). Although density data for the VDF/ CO_2 mixture is not readily available, the density of VDF/ CO_2 at 4000 psi (27.21 MPa) must be higher than under 1800 psi (12.24 MPa). Thus, it seems clear that at a lower density, the solubility of PVDF in the VDF/ CO_2 mixture is low. Under these conditions, the propagating macro-radical will aggregate or precipitate at a lower molecular weight. Additionally at lower pressure, the viscosity of the system will also be lower leading to a greater likelihood of termination by coupling. For all of these reasons, polymerisation at lower pressure results in a lower molecular weight and lower polymerisation rate; results that are in agreement with those of others [39].

4. Conclusion

The precipitation polymerisation of vinylidene fluoride in scCO_2 was monitored in situ by power compensation calorimetry. The polymer product was found to have a low apparent-density, leading to an observed high solid content in the autoclave at low yields. As a consequence, in situ calorimetry showed a sharp transition in the heat transfer in

the reactor, leading to a useful parameter for monitoring the polymerisation process. Our data demonstrate also the effects of stirring rate and pressure upon the progress of the PVDF precipitation polymerisation reaction in scCO_2 .

Acknowledgements

We thank Dr Wenxin Wang, Dr Jianyuan Hao and Mr Christopher J. Duxbury for scientific discussions and useful advice. We acknowledge the EC consortium ECOPOL (Contract No. G1RD-CT-2002-00676) for financial support (JL and HT). SMH is a Royal Society—Wolfson Research Merit Award Holder.

References

- [1] Scheinbeim JI. Poly(vinylidene fluoride). In: Mark JE, editor. Polymer data handbook. Oxford: Oxford University Press; 1999.
- [2] Banks RE, Smart BE, Tatlow JC. Organofluorine chemistry: principles and commercial applications. New York: Plenum; 1994.
- [3] Guiot J, Ameduri B, Boutevin B. *Macromolecules* 2002;35:8694–707.
- [4] Apostolo M, Arcella V, Storti G, Morbidelli M. *Macromolecules* 1999;32:989–1003.
- [5] Russo S, Behari K, Chengji S, Pianca M, Barchiesi E, Moggi G. *Polymer* 1993;34:4777–81.
- [6] Seiler DA. PVDF in the chemical process industry. In: Scheirs J, editor. *Modern fluoropolymers*. New York: Wiley; 1997.
- [7] Jessop PG, Leitner W. *Chemical synthesis using supercritical fluids*. Weinheim: Wiley-VCH; 1999.
- [8] McHugh MA, Krukonis VJ. *Supercritical fluid extraction: principles and practice*. Stoneham, MA: Butterworths; 1994.
- [9] Kendall JL, Canelas DA, Young JL, DeSimone JM. *Chem Rev* 1999; 99:543–63.
- [10] DeSimone JM, Maury EE, Menciloglu YZ, McClain JB, Romack TJ, Combes JR. *Science* 1994;265:356–9.
- [11] Cooper AI. *J Mater Chem* 2000;10:207–34.
- [12] Eckert CA, Knutson BL, Debenedetti PG. *Nature* 1996;383:313–8.
- [13] Charpentier PA, Kennedy KA, DeSimone JM, Roberts GW. *Macromolecules* 1999;32:5973–5.
- [14] Galia A, Caputo G, Spadaro G, Filardo G. *Ind Eng Chem Res* 2002; 41:5934–40.
- [15] Baradie B, Shoichet MS. *Macromolecules* 2002;35:3569–75.
- [16] Baradie B, Shoichet MS. *Macromolecules* 2003;36:2343–8.
- [17] Korber F, Hauschild K, Fink G. *Macromol Chem Phys* 2001;202: 3329–33.
- [18] BenAmor S, Colombie D, McKenna T. *Ind Eng Chem Res* 2002;41: 4233–41.

- [19] Wang WX, Griffiths RMT, Giles MR, Williams P, Howdle SM. *Eur Polym J* 2003;39:423–8.
- [20] Wang WX, Griffiths RMT, Naylor A, Giles MR, Irvine DJ, Howdle SM. *Polymer* 2002;43:6653–9.
- [21] Strain F, Bissinger WE, Dial WR, Rudolf H, DeWitt BJ, Stevens HC, Langston JH. *J Am Chem Soc* 1950;72:1254–63.
- [22] Furno F, Licence P, Howdle SM, Poliakoff M. *Actual Chim* 2003;62–6.
- [23] Christian P, Howdle SM, Irvine DJ. *Macromolecules* 2000;33:237–9.
- [24] Giles MR, Griffiths RMT, Aguiar-Ricardo A, Silva M, Howdle SM. *Macromolecules* 2001;34:20–5.
- [25] Charpentier PA, DeSimone JM, Roberts GW. *Chem Eng Sci* 2000;55:5341–9.
- [26] Zhang JX, Busby AJ, Roberts CJ, Chen XY, Davies MC, Tandler SJB, Howdle SM. *Macromolecules* 2002;35:8869–77.
- [27] Shenoy SL, Fujiwara T, Wynne KJ. *Macromolecules* 2003;36:3380–5.
- [28] Briscoe BJ, Lorge O, Wajs A, Dang P. *J Polym Sci Pt B-Polym Phys* 1998;36:2435–47.
- [29] Tai HY, Wang WX, Martin R, Liu J, Lester E, Licence P, Woods HM, Howdle SM. *Macromolecules*, 2005;38(1), in press.
- [30] Saraf MK, Gerard S, Wojcinski LM, Charpentier PA, DeSimone JM, Roberts GW. *Macromolecules* 2002;35:7976–85.
- [31] Kornfield JA, Kumaraswamy G, Issaian AM. *Ind Eng Chem Res* 2002;41:6383–92.
- [32] Acierno S, Palomba B, Winter HH, Grizzuti N. *Rheol Acta* 2003;42:243–50.
- [33] Bove L, Nobile MR. *Macromol Symp* 2002;185:135–47.
- [34] Somwangthanaroj A, Lee EC, Solomon MJ. *Macromolecules* 2003;36:2333–42.
- [35] Canelas DA, DeSimone JM. *Macromolecules* 1997;30:5673–82.
- [36] Shiho H, DeSimone JM. *Macromolecules* 2000;33:1565–9.
- [37] Shiho H, DeSimone JM. *J Polym Sci Pol Chem* 2000;38:3783–90.
- [38] Shiho H, DeSimone JM. *Macromolecules* 2001;34:1198–203.
- [39] Saraf MK, Wojcinski LM, Kennedy KA, Gerard S, Charpentier PA, DeSimone J, Roberts GW. *Macromol Symp* 2002;182:119–29.
- [40] Huang FH, Li MH, Lee LL, Starling KE, Chuang FTH. *J Chem Eng Jpn* 1985;18:490.